American Journal of Nano Research and Application
2014; 2(6-1): 9-18
Published online December 19, 2014 (http://www.sciencepublishinggroup.com/j/nano)
doi: 10.11648/j.nano.s.2014020601.12

Efficient route to high-quality graphene materials: Kinetically controlled electron beam induced reduction of graphene oxide in aqueous dispersion

Roman Flyunt[1, *], Wolfgang Knolle[1], Axel Kahnt[2], Siegfried Eigler[3], Andriy Lotnyk[1], Tilmann Häupl[1], Andrea Prager[1], Dirk Guldi[2], Bernd Abel[1]

[1]Leibniz-Institut für Oberflächenmodifizierung (IOM), Permoserstr. 15, 04303 Leipzig, Germany
[2]Department of Chemistry and Pharmacy & Interdisciplinary Center for Molecular Materials (ICMM), Friedrich-Alexander-Universität Erlangen-Nürnberg (FAU), Egerlandstraße 3, 91058 Erlangen, Germany
[3]Department of Chemistry and Pharmacy & Central Institute for New Materials and Processing Technology, Friedrich-Alexander-Universität Erlangen-Nürnberg (FAU), Dr.-Mack Str. 81, 90762 Fürth, Germany

Email address:
roman.flyunt@iom-leipzig.de (R. Flyunt)

To cite this article:
Roman Flyunt, Wolfgang Knolle, Axel Kahnt, Siegfried Eigler, Andriy Lotnyk, Tilmann Häupl, Andrea Prager, Dirk Guldi, Bernd Abel. Efficient Route to High-Quality Graphene Materials: Kinetically Controlled Electron Beam Induced Reduction of Graphene Oxide in Aqueous Dispersion. *American Journal of Nano Research and Application.* Special Issue: Advanced Functional Materials. Vol. 2, No. 6-1, 2014, pp. 9-18. doi: 10.11648/j.nano.s.2014020601.12

Abstract: This work is presenting a highly efficient, cost-efficient and environmentally friendly method for the production of graphene materials (reduced graphene oxide, RedGO) via electron beam (EB) irradiation of aqueous dispersions of graphene oxide (GO). Our strategy here is based on a reduction of GO via EB irradiation under optimally controlled conditions, i.e. dose and dose rate, reducing species, and taking the environmental impact of educt and product into account. The preparation of highly conductive RedGO under these conditions takes only 10-20 minutes at ambient temperature. After our first approach [1], a somewhat similar study was reported by Jung et *al.* [2] for GO dispersions in H_2O/EtOH (50:50). However, the latter route [2], although being similar in spirit, has serious drawbacks for large-scale production because of the formation of acetaldehyde, a very toxic compound, derived from the ethanol in the solvent. The advantages of the present approach compared to [2] are: (i) the use of water as a solvent with only a small content (0.03 - 2 wt.-%) of 2-PrOH allows the scaling-up, since neither 2-PrOH nor its final product acetone are of high technological or environmental concerns; (ii) a much lower dose is required for GO reduction (about 20 vs. 200 kGy, corresponding to only 1/10 of energy consumed); (iii) the conductivity of RedGO is over 60 times higher. Based on the XPS and conductivity measurements, it was established that the EB treatment is leading also to a more efficient reduction of GO compared to the hydrazine method. The highest conductivity in our systems is identical to the best known value of 3 x 10^4 S/m for RedGO obtained via HI / acetic acid treatment which takes, however, 40 h at 40 ºC.

Keywords: Electron Beam, Reducing Free Radicals, Reduced Graphene Oxide, Highly Conductive Carbon Nanomaterials, Graphene Oxide

1. Introduction

The discovery of graphene [3] is undoubtedly one of the most important events in the chemistry and physics of carbon materials within the past two decades. The chemistry and numerous applications of graphene, GO, and their derivatives are highlighted in recent reviews [4-10]. The most effective route to obtain low cost, good quality graphene in the form of highly reduced GO is through the reduction of GO (see eq.1) in its colloidal suspensions.

A number of conceptually different methods to reduce GO have been published, employing chemical reductants such as hydrazine, dimethylhydrazine, hydroquinone, $NaBH_4$, vitamine C, hydriodic/acetic acids, thermal means, and photocatalysis based on TiO_2 or ZnO etc. [8]. A detailed overview covering the most frequently used methods including a short discussion is given as Table 1. In chemical terms, reduction of GO is sketched in equation 1 for GO lacking major structural defects:

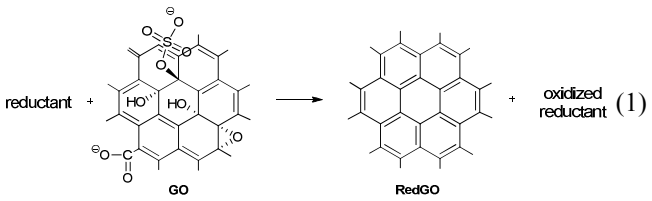

(1)

When comparing the different reduction processes a number of factors should be taken into account. The majority of recent investigations focuses on the quality of received RedGO as reflected in conductivity characteristics. Aspects like environmental hazard stemming from the reductant and/or its final product(s), on one hand, and process scalability, on the other hand, are, at least, of equal importance but are often neglected. The most important drawbacks of the well-known and favored reduction methods can be shortly summarized as follows. Firstly, a particular low conductivity is found for RedGO when hydroquinone, pyrogallol, KOH, or $NaBH_4$ are used. Secondly, reaction times reach up to 40 hours in the case of gamma irradiating GO dispersions, which is hardly acceptable. Thirdly, the toxicity of reducing agents such as hydrazine and hydroxylamine and their products is a problem. Fourthly, the highly explosive nature of hydrazine creates technological problems with respect to handling. Finally, the separation of the resulting RedGO from, for example, other components is also a big technological challenge, since vacuum filtration takes too long and waste disposal is too expensive. Zhang *et al.* [33] have investigated the γ-irradiation induced reduction of GO in dispersion. During reduction, the starting GO is subject to a significant deoxygenation, that is, transforming from a C/O ratio of 1.1 to 10.1, in N_2-purged H_2O/EtOH (1:1 v/v) solution. A distinct disadvantage of this approach is the

Table 1. *Comparison of the methods for the reduction of GO.*

Reducing compound or Method	Advantage	Disadvantage
Hydrazine [11-13]	very efficient	high temp. (95 ºC), hydrazine is explosive and highly toxic
Dimethylhydrazine [14]	very efficient	as for hydrazine
Hydroxylamine [15]	low price and lower toxicity compared to hydrazine	Explosive and toxic compound; slightly less efficient than hydrazine
Hydroquinone [16]	less toxic than hydrazine	much less efficient than hydrazine; 95 ºC
$NaBH_4$ [13, 17]	unknown	10^4 fold lower conductivity compared to hydrazine method, too expensive, 95 ºC
Pyrogallol [13]	less toxic than hydrazine	too expensive, 95 ºC
Hydriodic/acetic acid [18]	conductivity higher than for hydrazine method, treatment at 40 ºC	too expensive, too long process (40 h), waste management
$NaHSO_3$ and other sulfur-containing compounds [19]	cheap, low toxicity, conductivity is comparable with hydrazine method, duration 3 h	95 ºC; utilization of oxidation products derived from sulfur-containing compounds
vitamin C at 95 ºC [13]	short time (30 min), efficient almost as hydrazine, no toxicity	too expensive; 95 ºC; utilization of products from vitamin C;
vitamin C at room temperature [20]	no heating, no further oxidation processes	too long treatment (48 h), ~ 550 times lower conductivity compared to vitamin C at 95°C;
vitamin C + l-tryptophan [21]	gives a stable aqueous RedGO dispersion	even more expensive
vitamin C + Triton-X100 [22]	gives a stable aqueous RedGO dispersion	5 times lower conductivity than with vitamin C at 95 ºC
Aluminium powder [23]	Simple and fast reaction (30 min) without external heating; relatively low cost	5 times lower conductivity than that for the hydrazine method, product is in a form of precipitate; utilization of 0.5M HCl, Al and $AlCl_3$
Reduction at high pH [24]	Very fast (a few minutes at 50-80 ºC)	use of highly concentrated hydroxide; 5 x 10^4 fold lower conductivity compared to hydrazine method [13]
Thermal reduction [25, 26]	no need for dispersion in a solvent	1000º C; 30 % weight loss, graphene sheets highly wrinkled
Hydrothermal [27]	leads to a stable aqueous RedGO dispersion	180 ºC, 6 h, high content of oxygen in final product; no data on conductivity
Solvothermal [28]	good degree of deoxygenation, stable dispersion in propylene carbonate	150 ºC, conductivity is still 4 times lower compared to hydrazine method
Electrochemical reduction [29, 30]	very efficient, ambient temperature, no toxicity	high energy consumption; deposition of the product onto electrodes
TiO_2- or ZnO-assisted photocatalytical reduction [31, 32]	no toxicity, ambient temperature	only partial reduction; separation of graphene and semiconductor difficult due to deposition of the product on the photocatalyst
Gamma-irradiation of water-alcohol dispersions of GO [33]	Ambient temperature, low toxicity, high degree of deoxygenation, low costs	too long process (40 h), conductivity improvement (4-5 orders of magnitude) is still considerably lower compared to hydrazine method (6-7 orders)
EB treatment of water-alcohol dispersions of GO [2]	fast (20 minutes), ambient temperature	high dose of 200 kGy, moderate conductivity of RedGO, high toxicity of formed acetaldehyde

long irradiation time in the range of 40 h to realize a total absorbed energy of 35 kGy. In contrast to the latter, EB treatment generates free radicals in very high concentrations. Thus, short processing times and easy scalability become feasible.

It was recently demonstrated that the irradiation time can be significantly reduced to 5-20 minutes (corresponding to 50-200 kGy) by EB irradiation [2]. But, even with absorbed doses of 200 kGy the electrical characteristics of the correspondingly formed RedGO are still far from optimum when compared to benchmarks based on hydrazine or HI/AcOH treatment – vide infra. Moreover, the employed solvent was an ethanol-water mixture (1:1 v/v) [2, 33]. To this end, acetaldehyde is produced from ethanol, which poses high environment risks.

Very recently, we have reported a basic study on the radiation-induced reduction of GO, using water as solvent, where only small content (at most 2 wt.-%) of simple organic compounds are required to reduce GO [34]. In the current contribution, we demonstrate the highly efficient EB-induced reduction of GO with focus on its environmental compatibility, low cost, and scalability, and on overcoming the drawbacks described in any of the aforementioned approaches [2, 33]. It will be shown, that high quality RedGO with superior conductivity is obtained at much lower absorbed dose, using water containing ≤ 2 wt.-% of 2-PrOH. Importantly, acetone as the main product of the water / 2-PrOH radiolysis is of low environmental and technological concerns.

Three different samples of GO (from different suppliers) have been investigated to prove the general concept and to find out the peculiarities of each kind of GO. The study shows that the results strongly depend upon and vary with the initial material.

2. Experimental

All chemicals (Sigma-Aldrich) were of analytical grade and used without further purification.

Three different GO samples have been investigated in this work: a) single-layered GO purchased from Cheaptubes.com (USA; further called CT-GO), b) GO from Nanoinnova Technologies (Madrid, Spain; further called NT-GO) and c) home-made almost intact GO (further called ai-GO) synthesized according to Eigler *et al*. [35].

The aqueous 0.5 g/L GO solution was prepared by agitation in ultrasonic bath for 1 h, followed by vacuum filtration through *Millipore* HVLP *0.45 μm* membrane filter. The GO settled on the filter was then washed with copious amount of water and redispersed in Millipore water in ultrasonic bath for 15 min. The obtained GO solution with a natural pH of ca. 4.0 was then centrifuged at 4000 rpm for 4 hours. The decanted GO dispersion was used for described experiments. This procedure gives stable (> 1 month) dispersions of a few-layers GO as confirmed by TEM measurements with final concentration of 0.4 g/L. If needed, pH was adjusted with KOH solution. The preparation of stock solution of Nanoinnova Technologies GO (further NT-GO) was done in a similar manner, excepting much shorter ultracentrifugation time (a few times repeated ultracentrifugation for 15 min at 4000 rpm). This was due to much lower solubility (ca. 7-8 times) of NT-GO compared to CT-GO (final concentration is 0.05 g/L). The desired GO concentration was obtained by dilution of stock solution with Millipore water. Solubility of ai-GO is much higher due to the presence of organosulfate groups [36].

A stock solution (5 g/L of ai-GO) was diluted with Millipore water to a final GO concentration of 6.9 mg/L. This solution was divided into two equal aliquots. One was used at its original pH of 4, the pH of the second aliquot was adjusted to pH 10.

All GO solutions were purged with nitrogen (excepting the experiment with air-saturated solution) and irradiated with EB at 1 kGy/step. Irradiated solutions were vacuum filtrated (from Whatman, ∅ 47 mm, 0.2 μm pore size), washed with copious amount of Millipore water and dried in vacuum desiccator.

For the preparative irradiation of GO systems a 10 MeV linear accelerator ELEKTRONIKA (Toriy Company, Moscow) was employed, which is operating at 50 Hz repetition rate and 4μs pulse length.

Spectral changes in the EB-irradiated GO solutions were followed using UV-VIS spectrometer TIDAS-II (Spectralytics GmbH, Essingen, Germany).

TEM observations were performed with a probe Cs-corrected Titan^3 G2 60-300 microscope equipped with HAADF, BF, DF, ABF and Super-X EDX detectors as well as with GIF Quantum Gatan imaging filter. The microscope was operated at 80 kV to minimise sample damages.

Raman spectra were recorded from 1050 to 3410 cm^{-1} under 532 nm (2.33eV) excitation with two confocal microscope setups, a LabRAM ARAMIS (HORIBA Jobin Yvon) and an inverted microscope IX71 (Olympus) fiber coupled to a spectrometer (iHR320, synapse CCD, HORIBA Jobin Yvon). GO samples from Cheaptubes and Nanoinnova Technologies were measured dip coated on a silicon-oxide wafer (300 nm) with the former, vacuum filtrated ai-GO or ai-RedGO samples were performed with the latter setup.

XPS spectra were recorded on Axis Ultra (Kratos) using monochromatized Al-K_α radiation. Conductivity measurements of graphene-like materials were done on a MDC four-point probe system (MDC S.A, Geneve, Switzerland).

3. Results and Discussion

Irradiation of aqueous systems by EB generates three highly reactive radical species, namely hydrated electrons (e_{aq}^-), hydrogen atoms ($H^\bullet$), and hydroxyl radicals ($^\bullet OH$), as summarized in reaction 2 [37]:

$$H_2O \xrightarrow{\gamma-irradiation,\ electron\ beam} e_{aq}^-, H^\bullet, {}^\bullet OH, H_2O_2, H_{aq}^+, H_2 \quad (2)$$

The radiation chemical yields of the primary species amount to 0.6×10^{-7} mol J^{-1} for $H^\bullet$ and 2.9×10^{-7} mol J^{-1} for

e_{aq}^- and $^\bullet OH$. Both, e_{aq}^- and $H^\bullet$, are strong reductants with reduction potentials of –2.9 and –2.4 V, respectively [38] that are directly employable to reduce GO. In contrast, $^\bullet OH$ radicals are known as one of the strongest oxidants ($E(^\bullet OH, H^+/H_2O)$ = +2.73 V) [38] and, therefore, have to be converted into reducing radicals by a reaction with, for example, alcohols :

$$^\bullet OH + (CH_3)_2CHOH \rightarrow H_2O + (CH_3)_2{}^\bullet COH \quad (3)$$

Hydrogen atoms react with most alcohols in a similar manner to $^\bullet OH$ (reaction 3), giving the same reducing species. The reductants derived from simple alcohols such as 2-PrOH, EtOH, or MeOH feature reduction potentials of –1.9 V for $(CH_3)_2{}^\bullet C(OH)$, –1.25 V for $CH_3{}^\bullet CHOH$, and –1.18 V for $^\bullet CH_2OH$ [38]. As such, these values are comparable or even higher than those established for hydrazine (–1.16 V) or borohydride (–1.24 V) [23], known to efficiently reduce GO. Thus, the chosen free radical species are expected to render good reducing agents for GO as well.

The primary reductants e_{aq}^-, $H^\bullet$ and the secondary reductants – radicals formed via reaction 3 – react fast with oxygen with rate constants in the range of 10^9 - 10^{10} $dm^3\ mol^{-1}s^{-1}$) [37] to afford the corresponding peroxyl radicals. The latter are, however, unable to reduce GO. To avoid this undesired side reaction, it is favorable to conduct the irradiation of GO dispersions in the absence of oxygen. Thus, in N_2-saturated aqueous dispersions of GO in the presence of any of the aforementioned $^\bullet OH$-radical scavengers two major reductants, namely e_{aq}^- and radicals derived from the scavengers, are generated.

Upon EB irradiation in the presence of small amounts of MeOH, EtOH, or 2-PrOH, the initially yellow-brown aqueous GO dispersions turned black within a few minutes. Reduction of GO is easily followed employing UV-Vis spectroscopy. An example is given in Fig. 1 for the case of CT-GO and 2-PrOH as $^\bullet OH$-scavenger. The absorption maximum is shifting from ca. 227 nm for the starting GO to ca. 266 nm for the final RedGO. Similar trends evolved for NT-GO and ai-GO – Fig. 2 and 3. Shifts to 268 ± 2 nm after the reduction of GO with hydrazine and vitamin C (pH ~ 9-10) were reported in the literature [39, 40] and the resulting spectra were assigned to RedGO. Considering that the long-wavelength absorbance at $\lambda > 600$ nm is almost exclusively due to the absorption of RedGO – Fig. 1 – a rough estimate of the RedGO yield at a defined dose of EB irradiation is made with the maximum absorbance at, for example, 700 nm at hands. When comparing solutions containing 2 wt.-% of different OH scavengers, the highest absorbance was obtained in the EtOH system and taken as 100%. The corresponding values for aqueous dispersion with either 2-PrOH or MeOH at the same dose are 96 and 92%, respectively. Much lower values were derived for t-BuOH with 43%. In the latter, $^\bullet OH$ radicals are transformed into non-reducing species leaving electrons as the only reductants. In addition, we studied the reduction of GO with a number of other free radicals coming from the reaction of $^\bullet OH$ radicals with simple organics. Among those, formate is giving the same high yield of RedGO as EtOH, while ethylene glycol and glycerine afford somewhat smaller yields of 87 and 81%, respectively.

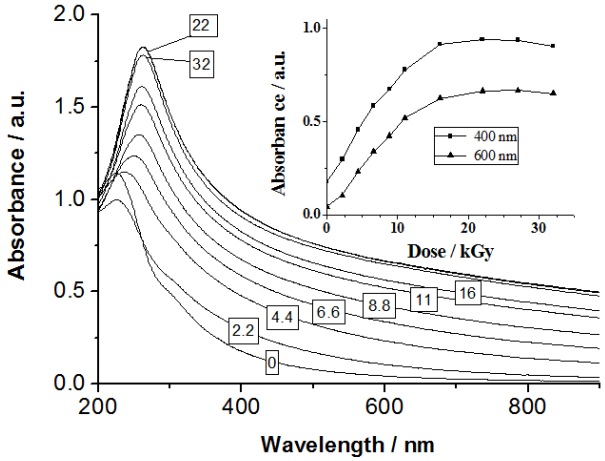

Figure 1. *UV-Vis spectra of EB-irradiated N_2-saturated solution containing 0.4 g/L CT-GO, 2 wt.-% 2-PrOH at pH 4. Absorbed doses are indicated in inset, irradiation followed in 1.1-1.2 kGy/step. Probes were diluted with water (1:9) before recording of spectra; Inset: absorbance bild-up at different wavelengths.*

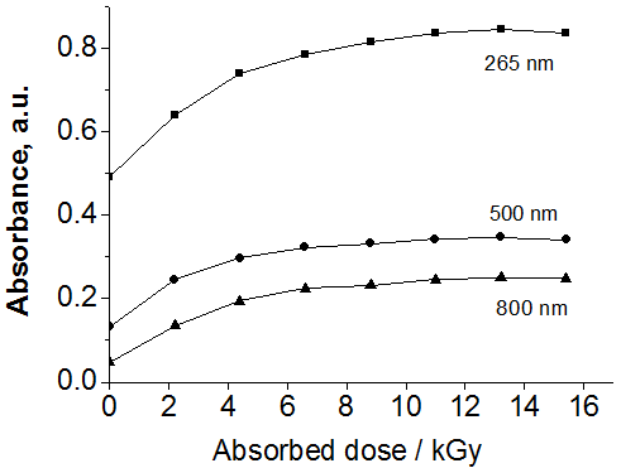

Figure 2. *Absorbance bild-up at different wavelengths during EB treatment of N_2-saturated solution containing NT-GO and 2 wt.-% iso-PrOH at pH 10.*

Other free radicals, which were formed from sucrose, glyoxylate and lactate are also able to reduce GO. But, the corresponding RedGO yields are significantly lower with 57% for sucrose, 42% for glyoxylate, and 40% for lactate. In conclusion, reducing radicals derived from MeOH, EtOH and 2-PrOH are most efficient in terms of GO reduction. To select any of them for industrial up-scaling, additional criteria are considered: on one hand, MeOH possesses incomparably higher toxicity than EtOH and 2-PrOH. On the other hand, formaldehyde and acetaldehyde, the final products of the radiolysis / reduction with MeOH and EtOH, respectively [37], are known to be very toxic, whereas acetone as it evolves from 2-PrOH (eq. 4) is neither a major environmental nor technological concern. Therefore, to up-scale the GO reduction, *the preference should be given to 2-*

PrOH. In this system, reduction of GO with $(CH_3)_2{}^{\bullet}C(OH)$ radicals follows:

$$n\ (CH_3)_2{}^{\bullet}C(OH) + GO \rightarrow n\ (CH_3)_2CO + RedGO + n\ H_2O \quad (4)$$

In competition to the desired reaction 4, $(CH_3)_2{}^{\bullet}C(OH)$ may undergo bimolecular termination reactions

$$2 \times (CH_3)_2C^{\bullet}(OH) \rightarrow products \quad (5)$$

Although the contribution of such unwanted reactions can be dramatically reduced by lowering the dose rate, the very low dose rates of, for example, gamma-irradiation results in an unacceptable long irradiation time [33]. High dose rates of 10 kGy/min as used in [2] will facilitate the termination reaction. In light of the latter and to realize optimum conditions, our experiments were performed at a dose rate of about 1 kGy/step.

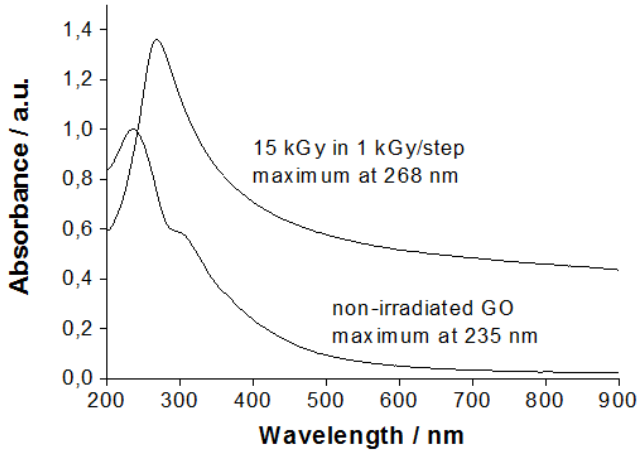

Figure 3. *UV-Vis spectra of aqueous dispersions of ai-GO at pH 10 (2 wt.-% 2-PrOH, N_2-sat.) before and after EB-treatment.*

It was established, that an efficient RedGO formation was also observed with much smaller concentration of $^{\bullet}OH$ scavengers. For example, decreasing EtOH from 2 to 0.03 wt.-% led to only a 15% shrinking of the RedGO yield at the same dose [34]. On a final note, EB-induced GO reduction is possible with an acceptable efficiency even in air-saturated solutions. We have found, that absorbance of the EB irradiated air-saturated solution of GO is only slightly lower (ca. 15 ± 5 %) compared to one for N_2-saturated solution in the whole UV-Vis spectrum. This is in a sharp contrast to gamma-irradiated GO [33], where almost no sign of GO reduction was seen in air-saturated solution. Dissolved oxygen (0.28 mM) is consumed via fast reactions with radical species after absorbance of ca. 1 kGy, i.e. in about 0.5 minute in our experiment and in appr. 1 h in the case of gamma-irradiation. Further diffusion of oxygen from the air into solution seems to be inefficient compared to GO reduction by means of EB, which is presumably the main reason for drastic difference observed for two methods. These aspects are advantageous for scaling-up.

The optimal dose for EB reduction of GO is determined by means of UV-Vis spectroscopy. As illustrated in Fig. 1, the absorbance from 200 to 900 nm maximizes at 22 kGy. Prolonged irradiation leads to an incremental decrease in absorbance. Considering, for example, spectra taken at 32 kGy, the effects are rationalized on grounds of RedGO agglomeration as described in [39].

In considering the ratio of absorbancies for RedGO and GO, namely A_{RedGO}/A_{GO}, we established a simple UV spectroscopic criterion to relate to the degree of GO reduction in aqueous solutions. For EB treated CT-GO it is 1.6. Control experiments, in which the GO solutions were reduced with hydrazine gave identical values for λ_{max}, A_{RedGO} and A_{RedGO}/A_{GO}. Similar A_{RedGO}/A_{GO} ratios in the range from 1.5 to 1.6 were calculated from the data reported in [39] and [40]. The values obtained for NT-GO and ai-GO are slightly lower with 1.45 and 1.35, respectively, in the latter case precipitation sets in.

To this date, Raman spectra of RedGO are interpreted in different, sometimes controversial ways. Based on a recent work [41], we applied Lorentz functions to fit the obtained Raman spectra. Overall, they reveal the characteristics of few-layer-graphene with broadened D and G bands. They were deconvoluted into D, D** and G bands – Fig. 4. Contributions stemming from D* and D´ bands were, however, negligible. It should be noted that the Raman spectra of ai-GO samples were fit satisfactory without the needs of adding D** bands to the deconvolution routine. Similarly, the so-called 2 D regions in the Raman spectra were fit with three peaks located at around 2690 ± 30, 2940 ± 30, and 3200 ± 30 cm^{-1} – Fig. 4 and Table 2 – which are assigned to 2 D (or G´), D + D´ and 2 D´ modes, respectively. All bands in the 2 D region are markedly broadened. As a matter of fact this is typical for batches featuring sufficient numbers of defects.

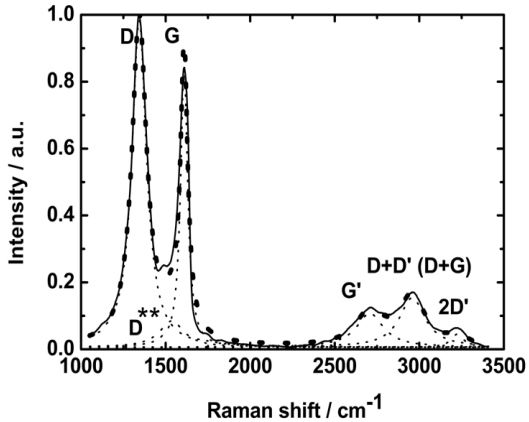

Figure 4. *Raman spectrum of RedGO obtained after EB treatment of CT-GO dispersion at pH 10 (solid line) and the deconvoluted (thin dashed line) and fitted (thick dashed line) spectra. To note: all presented Raman spectra (Fig. 4 - Fig. 6) are normalised taking the intensity of D band as unity.*

From our Raman measurements we conclude that the D and G bands sharpen considerably upon reduction – see Fig. 5, 6 and Table 2). This effect is quantified by the full width at half maximum (FWHM) values denoted as Γ. Especially pronounced is a drop of Γ_D for ai-GO from 134 to about 75

cm^{-1} prior and after its reduction, respectively – Table 2. In contrast, the G band sharpening is rather moderate with an initial Γ_G of ca. 85 cm^{-1} and a final Γ_G of ca. 65 ± 4 cm^{-1}. A sharpening of the Raman spectra of RedGO correlates with an increased quality. Earlier investigations on ai-GO were performed exclusively with films of single flakes, while Raman spectra of few-layer and multi-layer graphene have been filtered out [35, 42, 43]. In the present study, we analyze, however, the complete sample reduced in dispersion followed by filtration.

D bands of treated GO are usually downshifted compared to the non-treated one (see Table 2). For example, in the case of CT-GO, the D band has maxima at 1344 cm^{-1} for EB and hydrazine treated solution and at 1353 cm^{-1} for the starting GO. The maxima for D bands for all irradiated ai-GO probes are situated at 1332-33 cm^{-1}, which is about 15 cm^{-1} downshifted compared to non-treated sample. A different picture was observed for hydrazine treated ai-GO, namely there is almost no shift of the D band (1346 vs 1348 cm^{-1}). Non-treated and irradiated samples NT-GO have the same maxima positions for D band as well.

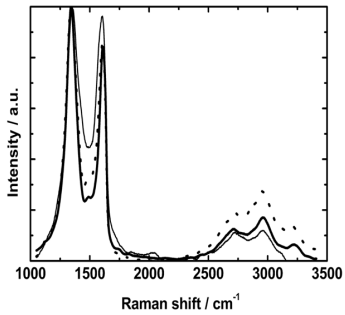

Figure 5. *Raman spectra of CT-GO (thin grey line curve) and RedGO obtained after hydrazine (dashed line curve) and EB-treatment (thick line curve).*

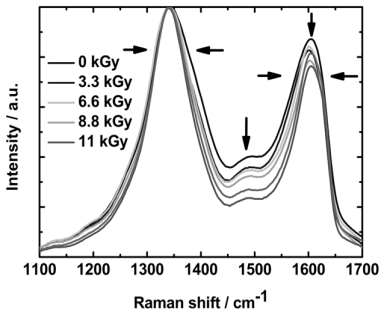

Figure 6. *Raman spectra of NT-GO before and after EB-irradiation.*

Table 2. *Results of Raman analysis for GO and RedGO*

Band assignment/Ratios of intensities	**D**	**D****	**G**	**2D**	**D + D´**	**2 D'**	**A_D/A_G**
CT-GO *non-treated*							
Peak maxima / cm^{-1}	1353	1490	1598	2725	2966	3230	1.77
Γ, cm^{-1}	128	155	75	222	177	208	
EB treated							
Peak maxima / cm^{-1}	1344	1541	1610	2708	2958	3225	2.36
Γ, cm^{-1}	105	134	51	196	194	84	
hydrazine treated							
Peak maxima / cm^{-1}	1344	1525	1604	2708	2954	3222	2.48
Γ, cm^{-1}	113	109	55	225	224	193	
NT-GO *non-treated*							
Peak maxima / cm^{-1}	1344	1535	1606	2719	2950	3207	2.2
Γ, cm^{-1}	118	120	63	339	218	253	
EB treated							
Peak maxima / cm^{-1}	1344	1520	1603	2713	2956	3227	2.4
Γ, cm^{-1}	104	120	54	256	219	246	
ai-GO non-treated							
Peak maxima / cm^{-1}	1348	n.u.*	1588	2681	2926	3171	1.68
Γ, cm^{-1}	135	-	85	262	182	51	
ai-GO hydrazine treated							
Peak maxima / cm^{-1}	1346	n.u.*	1594	2681	2939	3189	1.96
Γ, cm^{-1}	77	-	68	216	148	148	
ai-GO pH 10, EB treated							
Peak maxima / cm^{-1}	1333	n.u.*	1585	2676	2923	3187	1.94
Γ, cm^{-1}	74	-	65	148	127	92	

* - the Raman spectra of ai-GO samples were fitted satisfactory without the use of D** band.

Usually, a downshift for G band of RedGO is associated with restoration of the hexagonal network of conjugated sp2 C-C bonds. In contrast, an upshift for G band is attributed to the formation of isolated C=C bonds [44]. It should be, however, noted that a typical error for the Raman measurements is equal to ± 4 cm-1, so the observed small shifts have to be taken with precaution.

With the measured D and G peak areas in hand the values of AD/AG as a measure of the lattice disorder [45] have been calculated. In the case of CT-GO samples, they were equal to 1.77, 2.36 and 2.48 for starting GO, EB treated GO, and hydrazine treated GO, respectively. Weaker were the increases of the A_D/A_G ratio for NT-GO (ca. 8%) and ai-GO samples (at most 15%). From the fact that EB and hydrazine

treated samples give similar A_D/A_G ratios we conclude that both methods are comparable. An increase in the I_D/I_G ratio upon treatment with a variety of reductants is well documented in the literature [11, 33, 46-48]. In the current study we used the A_D/A_G ratio rather than the I_D/I_G ratio, owing to the fact that peaks with different line width are compared. Overall, this effect is rationalized by decreasing sizes of in-plane sp^2-domains of graphene as well as partially ordered crystal structures of RedGO [44]. The lower A_D/A_G ratios as they were observed for treated ai-GO relative to CT-GO and NT-GO samples, infers that the former is of better quality with a lower defect density.

Fig. 7a illustrates a bright-field TEM image of CT-GO sample. As such, the sheet contains defects like holes – Fig. 7a, bottom left. A selected area electron diffraction (SAED) pattern of GO is shown in Fig. 7b. In the latter, the measured d-spacing indicates graphitic crystalline structures of GO, which was further corroborated by electron energy loss spectroscopy (EELS) investigations – Fig. 8.

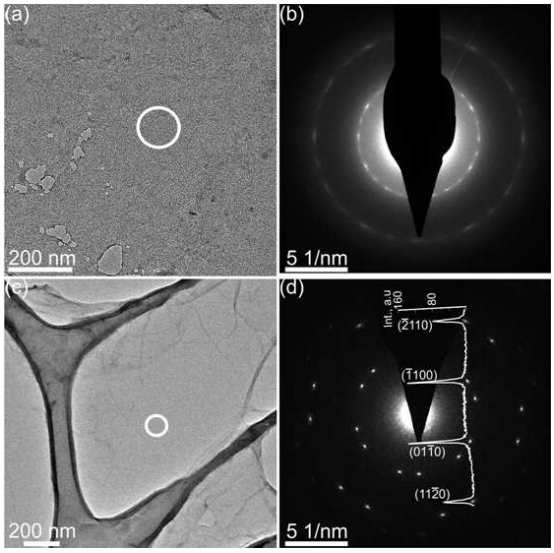

Figure 7. *TEM images of (a) GO and (c) RedGO. SAED patterns of (b) GO and (d) RedGO. The patterns were taken from the areas marked by the white circles in images (a) and (c). All measurements were done with CT-GO.*

However, the ring-shaped pattern consisting of many diffraction spots suggests multilayer structure of starting GO. The average thickness of the GO specimen based on EELS measurements ranged from 2.3 to 9 nm and is approximated as 2 to 8 layers. In stark contrast, a bright-field TEM image of a RedGO specimen – Fig 7c –, reveals wrinkling and folding of the RedGO sheet. In a typical SAED pattern of the RedGO sample – Fig. 7d – the slight spot broadening in the pattern is due to the fact that the RedGO sheets are not exactly flat [49]. Additionally, analysis of diffracted intensities of the SAED pattern in Fig. 7d confirmed the bilayer structure of the RedGO sheet [49, 50], a representative one for this sample. The profile along the (-2110) to the (-1120) reflections gives ratios of $I_{\{1110\}}/I_{\{2110\}}$ close to 1.8. Notably, ratios larger than 1 indicate single layer graphene structures [49, 50]. A quantitative similar behavior of $I_{\{1110\}}/I_{\{2110\}}$ was observed for all others diffracted intensities in Fig. 7d. Thus, the RedGO sheet is two layers thick. Measurements of thickness on different sample areas using EELS resulted in thicknesses of RedGO sheets in the range from 2 to 4 nm, that is approximately 2 to 4 layers. At this point we hypothesize that further exfoliation took place during the EB induced GO reduction.

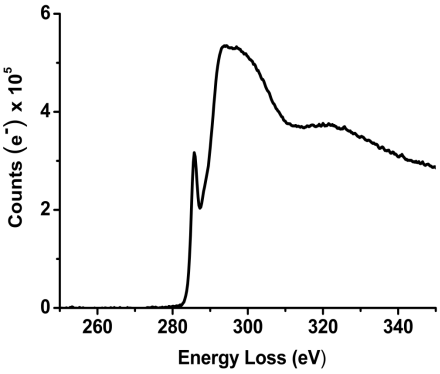

Figure 8. *EELS spectra of C K-edge taken from CT-GO.*

Reduction of GO under EB irradiation is clearly confirmed by XPS. The two main peaks in the XPS spectrum of the starting ai-GO – Fig. 9 – are situated at 284.5 and 286.5 eV with a relative distribution of 48 and 52%, respectively. Upon GO reduction, the relative intensity of the first peak strongly increased, whereas that of the second peak dramatically decreased. In the deconvoluted XPS spectra of ai-RedGO obtained via EB treatment – inset to Fig. 9 – the contributions of C-C sp^2 at 284.6 eV, C-OH at 285.1 eV, epoxy/ether at 286.1 eV, C=O at 287.2 eV, and carboxyl at 289.1 eV are discernable.

XPS analyses shed light onto the C/O ratios, which increased from 2.60 for ai-GO prior to EB treatment to 10.9 (pH 4) and 9.6 (pH 10), respectively, after EB treatment. Any of these values are higher than the 7.1 obtained for the hydrazine treated ai-GO - Table 3. Additionally, the intensity of the C1 peak due to C-C sp^2 is higher and the intensities of the other peaks are lower for the EB method – Fig. 9. Based on these findings, one can state that the EB treatment is leading to a more efficient reduction of GO compared to the hydrazine method.

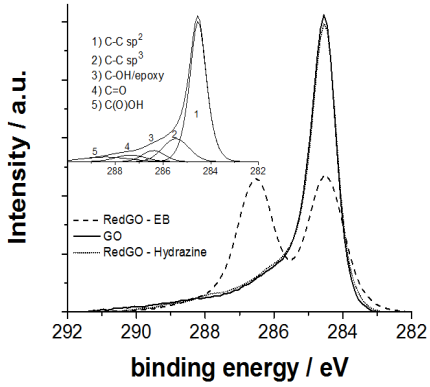

Figure 9. *Core level C1s XPS spectra of ai-GO (dashed line) and ai-RedGO obtained by its treatment with hydrazine (dotted line) and EB (full line). Inset: curve fit of XPS spectrum of ai-RedGO (EB method).*

The highest conductivity of 29000 S/m was seen for the ai-GO with pH 10. The RedGO film obtained from the same GO, but reduced at pH 4, gives rise to a 5 times lower conductivity of 5400 S/m. This indicates that GO at pH 10, where the carboxylic groups (pK_a = 6.1) are fully deprotonated [39], is more susceptible for reduction. A likely factor is a higher degree of exfoliation of ai-GO at pH 10 due to a strong electrostatic repulsion of the GO sheets with completely dissociated carboxylic groups.

These results underline that deoxygenation of GO is necessary but not decisive to obtain highly conductive RedGO. The conductivity of RedGO depends not only on the reduction conditions and more efforts are needed to map out this aspect with sufficient care. The nature of a GO sample, that is, the kind and density of defects, the lateral sizes of sheets, the presence of impurities, etc. plays a large role. As it is illustrated in Table 3, the conductivity of RedGO from CT-GO is low compared to ai-RedGO. It should be noted that the highest conductivity measured in this study is 2.9 x 10^4 S/m for ai-GO at pH 10 which, in turn, is more than 60 times higher than the reported 450 S/m for RedGO obtained by EB treatment of GO dispersions in H_2O/EtOH (1:1) [2]. It should also be recognized that the dose applied in our experiments is nearly 10 times lower – 22 versus 200 kGy – which infers the needs for much lower energy input. Another important advantage is the use of H_2O/2-PrOH (98:2 v/v) as solvent instead of H_2O/EtOH (50:50 v/v) enabling the scale-up as discussed above. Importantly, the highest conductivity in our study is identical to the best known value for RedGO obtained with HI-acetic acid method [48]. However, the latter requires 40 h treatment at 40 ºC. It is interesting to note that the conductivity of films made of graphene nanoplatelets is only two times higher (6 x 10^4 S/m) [51].

Table 3. *Conductivity and C/O ratio measurements for different RedGO probes.*

Probe and conditions	Conductivity, S/m	Measured C/O ratio*
ai-GO, pH 4, 15 kGy	5400	10.9
ai-GO, pH 10, 15 kGy	29000	9.6
hydrazine treated ai-GO, pH 10	14000	7.1
CT-GO pH 10, 22 kGy	480	7.3
EB treated GO in H_2O:EtOH (1:1), at 50 kGy/200 kGy [2]	1.5 / 450	not reported
HI/acetic acid treated GO (40 h at 40 °C) [48]	30000	6.7

* - the calculated C/O ratios represent a lower limit values. A certain amount of oxygen originates from of Si and S compounds which were detected in the range of a few percents. However, as their stoichiometry with oxygen is unknown, a correction for the C/O ratio is unreliable.

Our present study reveals the great potential of EB reduction of GO for the preparation of RedGO, with a conductivity well comparable with the best known wet-chemical methods.

In conclusion, we highlighted a rational synthesis strategy, appreciating the advantages of high energy radiation to provide optimal reduction conditions, which appears to be superior to other approaches lacking options in terms of environmentally friendliness, cost-effectiveness, and up-scaling for a high quality graphene material.

Acknowledgments

The financial support of the European Union and the Free State of Saxony (LenA project) is greatly acknowledged. AK, BA and DG are gratefully acknowledging funding from the Deutsche Forschungsgemeinschaft (DFG) via grants KA 3491/2-1/AB 63/14-1 and EI 938/3-1. We like to thank Dr. Jenny Malig for her support during the Raman measurements. We thank Prof. Dr. Andreas Hirsch for his support at FAU Erlangen-Nürnberg. This work is also supported by the Cluster of Excellence 'Engineering of Advanced Materials (EAM)' and SFB 953 funded by the DFG.

References

[1] R. Flyunt, W. Knolle, B. Abel, B. Rauschenbach, Verfahren zur Herstellung von reduziertem Graphenoxid sowie damit hergestelltes reduziertes Graphenoxid und dessen Verwendung 2012.

[2] J.-M. Jung, C.-H. Jung, M.-S. Oh, I.-T. Hwang, C.-H. Jung, K. Shin, J. Hwang, S.-H. Park, J.-H. Choi, Rapid, facile, and eco-friendly reduction of graphene oxide by electron beam irradiation in an alcohol–water solution, Materials Letters, 126 (2014) 151-153.

[3] K.S. Novoselov, A.K. Geim, S.V. Morozov, D. Jiang, Y. Zhang, S.V. Dubonos, I.V. Grigorieva, A.A. Firsov, Electric field effect in atomically thin carbon films, Science, 306 (2004) 666-669.

[4] S. Park, R.S. Ruoff, Chemical methods for the production of graphenes, Nature Nanotechnology, 4 (2009) 217-224.

[5] O.C. Compton, S.T. Nguyen, Graphene Oxide, Highly Reduced Graphene Oxide, and Graphene: Versatile Building Blocks for Carbon-Based Materials, Small, 6 (2010) 711-723.

[6] D.R. Dreyer, S. Park, C.W. Bielawski, R.S. Ruoff, The chemistry of graphene oxide, Chemical Society Reviews, 39 (2010) 228-240.

[7] H. Kim, A.A. Abdala, C.W. Macosko, Graphene/Polymer Nanocomposites, Macromolecules, 43 (2010) 6515-6530.

[8] C.K. Chua, M. Pumera, Chemical reduction of graphene oxide: a synthetic chemistry viewpoint, Chemical Society Reviews, 43 (2014) 291-312.

[9] S.F. Pei, H.M. Cheng, The reduction of graphene oxide, Carbon, 50 (2012) 3210-3228.

[10] S. Eigler, A. Hirsch, Chemistry with Graphene and graphene oxide - challenges for synthetic chemists, Angewandte Chemie International Edition, (2014).

[11] S. Stankovich, D.A. Dikin, R.D. Piner, K.A. Kohlhaas, A. Kleinhammes, Y. Jia, Y. Wu, S.T. Nguyen, R.S. Ruoff, Synthesis of graphene-based nanosheets via chemical reduction of exfoliated graphite oxide, Carbon, 45 (2007) 1558-1565.

[12] C. Gomez-Navarro, R.T. Weitz, A.M. Bittner, M. Scolari, A. Mews, M. Burghard, K. Kern, Electronic transport properties of individual chemically reduced graphene oxide sheets, Nano Letters, 7 (2007) 3499-3503.

[13] M.J. Fernandez-Merino, L. Guardia, J.I. Paredes, S. Villar-Rodil, P. Solis-Fernandez, A. Martinez-Alonso, J.M.D. Tascon, Vitamin C Is an Ideal Substitute for Hydrazine in the Reduction of Graphene Oxide Suspensions, Journal of Physical Chemistry C, 114 (2010) 6426-6432.

[14] S. Stankovich, D.A. Dikin, G.H.B. Dommett, K.M. Kohlhaas, E.J. Zimney, E.A. Stach, R.D. Piner, S.T. Nguyen, R.S. Ruoff, Graphene-based composite materials, Nature, 442 (2006) 282-286.

[15] X.J. Zhou, J.L. Zhang, H.X. Wu, H.J. Yang, J.Y. Zhang, S.W. Guo, Reducing Graphene Oxide via Hydroxylamine: A Simple and Efficient Route to Graphene, Journal of Physical Chemistry C, 115 (2011) 11957-11961.

[16] G.X. Wang, J. Yang, J. Park, X.L. Gou, B. Wang, H. Liu, J. Yao, Facile synthesis and characterization of graphene nanosheets, Journal of Physical Chemistry C, 112 (2008) 8192-8195.

[17] Y. Si, E.T. Samulski, Synthesis of water soluble graphene, Nano Letters, 8 (2008) 1679-1682.

[18] I.K. Moon, J. Lee, R.S. Ruoff, H. Lee, Reduced graphene oxide by chemical graphitization, Nat Commun, 1 (2010) 73.

[19] W.F. Chen, L.F. Yan, P.R. Bangal, Chemical Reduction of Graphene Oxide to Graphene by Sulfur-Containing Compounds, Journal of Physical Chemistry C, 114 (2010) 19885-19890.

[20] J. Zhang, H. Yang, G. Shen, P. Cheng, J. Zhang, S. Guo, Reduction of graphene oxide via L-ascorbic acid, Chem Commun, 46 (2010) 1112-1114.

[21] J. Gao, F. Liu, Y.L. Liu, N. Ma, Z.Q. Wang, X. Zhang, Environment-Friendly Method To Produce Graphene That Employs Vitamin C and Amino Acid, Chemistry of Materials, 22 (2010) 2213-2218.

[22] V. Dua, S.P. Surwade, S. Ammu, S.R. Agnihotra, S. Jain, K.E. Roberts, S. Park, R.S. Ruoff, S.K. Manohar, All-Organic Vapor Sensor Using Inkjet-Printed Reduced Graphene Oxide, Angewandte Chemie International Edition, 49 (2010) 2154-2157.

[23] Z.J. Fan, K. Wang, T. Wei, J. Yan, L.P. Song, B. Shao, An environmentally friendly and efficient route for the reduction of graphene oxide by aluminum powder, Carbon, 48 (2010) 1686-1689.

[24] X. Fan, W. Peng, Y. Li, X. Li, S. Wang, G. Zhang, F. Zhang, Deoxygenation of Exfoliated Graphite Oxide under Alkaline Conditions: A Green Route to Graphene Preparation, Adv Mater, 20 (2008) 4490-4493.

[25] M.J. McAllister, J.L. Li, D.H. Adamson, H.C. Schniepp, A.A. Abdala, J. Liu, M. Herrera-Alonso, D.L. Milius, R. Car, R.K. Prud'homme, I.A. Aksay, Single sheet functionalized graphene by oxidation and thermal expansion of graphite, Chemistry of Materials, 19 (2007) 4396-4404.

[26] P. Steurer, R. Wissert, R. Thomann, R. Mulhaupt, Functionalized Graphenes and Thermoplastic Nanocomposites Based upon Expanded Graphite Oxide, Macromolecular Rapid Communications, 30 (2009) 316-327.

[27] Y. Zhou, Q. Bao, L.A.L. Tang, Y. Zhong, K.P. Loh, Hydrothermal Dehydration for the "Green" Reduction of Exfoliated Graphene Oxide to Graphene and Demonstration of Tunable Optical Limiting Properties, Chemistry of Materials, 21 (2009) 2950-2956.

[28] Y.W. Zhu, M.D. Stoller, W.W. Cai, A. Velamakanni, R.D. Piner, D. Chen, R.S. Ruoff, Exfoliation of Graphite Oxide in Propylene Carbonate and Thermal Reduction of the Resulting Graphene Oxide Platelets, Acs Nano, 4 (2010) 1227-1233.

[29] M. Zhou, Y.L. Wang, Y.M. Zhai, J.F. Zhai, W. Ren, F.A. Wang, S.J. Dong, Controlled Synthesis of Large-Area and Patterned Electrochemically Reduced Graphene Oxide Films, Chem-Eur J, 15 (2009) 6116-6120.

[30] R.S. Sundaram, C. Gomez-Navarro, K. Balasubramanian, M. Burghard, K. Kern, Electrochemical modification of graphene, Adv Mater, 20 (2008) 3050-3053.

[31] G. Williams, P.V. Kamat, Graphene-Semiconductor Nanocomposites: Excited-State Interactions between ZnO Nanoparticles and Graphene Oxide, Langmuir, 25 (2009) 13869-13873.

[32] G. Williams, B. Seger, P.V. Kamat, TiO_2-graphene nanocomposites. UV-assisted photocatalytic reduction of graphene oxide, Acs Nano, 2 (2008) 1487-1491.

[33] B. Zhang, L. Li, Z. Wang, S. Xie, Y. Zhang, Y. Shen, M. Yu, B. Deng, Q. Huang, C. Fan, J. Li, Radiation induced reduction: an effective and clean route to synthesize functionalized graphene, Journal of Materials Chemistry, 22 (2012) 7775-7781.

[34] R. Flyunt, W. Knolle, A. Kahnt, A. Prager, A. Lotnyk, J. Malig, D. Guldi, A. Abel, Mechanistic Aspects of the Radiation-Chemical Reduction of Graphene Oxide to Graphene-Like Materials International Journal of Radiation Biology, 90 (2014) 486-494.

[35] S. Eigler, M. Enzelberger-Heim, S. Grimm, P. Hofmann, W. Kroener, A. Geworski, C. Dotzer, M. Rockert, J. Xiao, C. Papp, O. Lytken, H.P. Steinruck, P. Muller, A. Hirsch, Wet Chemical Synthesis of Graphene, Adv Mater, 25 (2013) 3583-3587.

[36] S. Eigler, C. Dotzer, F. Hof, W. Bauer, A. Hirsch, Sulfur Species in Graphene Oxide, Chem-Eur J, 19 (2013) 9490-9496.

[37] G.V. Buxton, C.L. Greenstock, W.P. Helman, A.B. Ross, Critical-Review of Rate Constants for Reactions of Hydrated Electrons, Hydrogen-Atoms and Hydroxyl Radicals (°OH/°O^-) in Aqueous-Solution, Journal of Physical and Chemical Reference Data, 17 (1988) 513-886.

[38] P. Wardman, Reduction Potentials of One-Electron Couples Involving Free-Radicals in Aqueous-Solution, Journal of Physical and Chemical Reference Data, 18 (1989) 1637-1755.

[39] D. Li, M.B. Muller, S. Gilje, R.B. Kaner, G.G. Wallace, Processable aqueous dispersions of graphene nanosheets, Nature Nanotechnology, 3 (2008) 101-105.

[40] J.I. Paredes, S. Villar-Rodil, P. Solis-Fernandez, A. Martinez-Alonso, J.M.D. Tascon, Atomic Force and Scanning Tunneling Microscopy Imaging of Graphene Nanosheets Derived from Graphite Oxide, Langmuir, 25 (2009) 5957-5968.

[41] A. Kaniyoor, S. Ramaprabhu, A Raman spectroscopic investigation of graphite oxide derived graphene, Aip Adv, 2 (2012).

[42] S. Eigler, S. Grimm, M. Enzelberger-Heim, P. Muller, A. Hirsch, Graphene oxide: efficiency of reducing agents, Chem Commun, 49 (2013) 7391-7393.

[43] S. Eigler, F. Hof, M. Enzelberger-Heim, S. Grimm, P. Müller, A. Hirsch, Statistical Raman Microscopy and Atomic Force Microscopy on Heterogeneous Graphene Obtained after Reduction of Graphene Oxide, The Journal of Physical Chemistry C, 118 (2014) 7698-7704.

[44] A.C. Ferrari, J. Robertson, Interpretation of Raman spectra of disordered and amorphous carbon, Phys Rev B, 61 (2000) 14095-14107.

[45] M.M. Lucchese, F. Stavale, E.H.M. Ferreira, C. Vilani, M.V.O. Moutinho, R.B. Capaz, C.A. Achete, A. Jorio, Quantifying ion-induced defects and Raman relaxation length in graphene, Carbon, 48 (2010) 1592-1597.

[46] V.H. Pham, H.D. Pham, T.T. Dang, S.H. Hur, E.J. Kim, B.S. Kong, S. Kim, J.S. Chung, Chemical reduction of an aqueous suspension of graphene oxide by nascent hydrogen, Journal of Materials Chemistry, 22 (2012) 10530-10536.

[47] Y.X. Xu, K.X. Sheng, C. Li, G.Q. Shi, Highly conductive chemically converted graphene prepared from mildly oxidized graphene oxide, Journal of Materials Chemistry, 21 (2011) 7376-7380.

[48] I.K. Moon, J. Lee, R.S. Ruoff, H. Lee, Reduced graphene oxide by chemical graphitization, Nat Commun, 1 (2010).

[49] J.C. Meyer, A.K. Geim, M.I. Katsnelson, K.S. Novoselov, D. Obergfell, S. Roth, C. Girit, A. Zettl, On the roughness of single- and bi-layer graphene membranes, Solid State Commun, 143 (2007) 101-109.

[50] Y. Hernandez, V. Nicolosi, M. Lotya, F.M. Blighe, Z.Y. Sun, S. De, I.T. McGovern, B. Holland, M. Byrne, Y.K. Gun'ko, J.J. Boland, P. Niraj, G. Duesberg, S. Krishnamurthy, R. Goodhue, J. Hutchison, V. Scardaci, A.C. Ferrari, J.N. Coleman, High-yield production of graphene by liquid-phase exfoliation of graphite, Nature Nanotechnology, 3 (2008) 563-568.

[51] Y. Geng, S.J. Wang, J.-K. Kim, Preparation of graphite nanoplatelets and graphene sheets, Journal of Colloid and Interface Science, 336 (2009) 592-598.